Journal of Microwaves, Optoelectronics and Electromagnetic Applications, Vol. 18, No. 2, June 2019
DOI: http://dx.doi.org/10.1590/2179-10742019v18i21550

Synthesis of New Reconfigurable Limited Size FSS Structures Using an Improved Hybrid Particle Swarm Optimization

Patric Lacouth[1,2], Adaildo Gomes D'Assunção[2], Alfrêdo Gomes Neto[1]
[1]*Federal Institute of Paraíba, Av. João da Mata 256, Jaguaribe, CEP: 58015-430, João Pessoa, PB, Brazil. patric.silva@ifpb.edu.br, alfredogomes@ieee.org*
[2]*Federal University of Rio Grande do Norte, Department of Communication Engineering, Caixa Postal 1655, CEP: 59072-970, Natal, RN, Brazil, adaildo@ct.ufrn.br*

***Abstract*— This paper describes a new design methodology for reconfigurable printed circuits with limited size, using an improved hybrid particle swarm optimization (HPSO) algorithm, reducing the search space by the definition of negative zones (NZ), regions where the swarm of particles should not travel. The proposed design methodology (HPSO-NZ) is used in the development of reconfigurable frequency selective surfaces (RFSSs), restricted to a limited overall size, resulting in entirely new frequency selective surface (FSS) geometries. Two FSS prototypes are designed, fabricated, and measured for comparison purpose. A good agreement is observed between simulation and measurements results, confirming the efficiency and accuracy of the HPSO-NZ algorithm. Also, the performance of the HPSO-NZ algorithm is compared to the ones of genetic algorithm (GA) and particle swarm optimization (PSO) algorithm, showing good consistency results.**

***Index Terms*—** *Particle swarm optimization, PSO, negative zones, HPSO-NZ, GA, reconfigurable FSS.*

I. INTRODUCTION

Wireless communication systems are evolving to a new generation of multifunctional platforms that offer high-quality services that demand high data transmission rates such as global positioning system (GPS) applications, video, and audio transmissions, internet and others. All these services require the development of devices and circuits capable of adapting to different conditions of transmission rate, interference, and fading [1].

These new radio systems necessarily will require the development of devices such as antennas, filters and feeding line circuits which are capable of operating in different frequency bands and intensity. The reconfiguration of an antenna or microwave circuit is achieved by a deliberate change in its operating

Brazilian Microwave and Optoelectronics Society-SBMO *received 22 Nov 2018; for review 22 Nov 2018; accepted 25 Feb 2019*
Brazilian Society of Electromagnetism-SBMag *ISSN 2179-1074*

frequency, polarization or radiation characteristics [2]. This change can be obtained by different techniques redistributing the electrical current density of the antenna and modifying its radiation pattern.

Recently, it is observed a high interest in the development of reconfigurable and compact printed circuits because of their ease integration to small equipment and ability to operate in different frequencies according to the communication system requirements. The performance of many radio-based communications systems can be significantly improved by using small and reconfigurable integrated circuits.

The design process and development of reconfigurable printed circuits require the appropriate integration of different components in the structure, such as radio frequency microelectromechanical system (RF MEMS), PIN diodes, and varactors, among others, on the surface of the printed circuit or feeding lines. Indeed, this is a real challenge since it is necessary to consider all the influences caused by switching components and activation lines in the final frequency response of the printed circuit [3].

Frequency selective surfaces (FSSs) are periodic structures interacting with electromagnetic (EM) waves to provide resonant frequencies selectivity [4]. FSSs were successfully introduced in antenna designs for several purposes such as suppressing surface waves and achieving low profile patch antennas and switched-beam antennas [5]. Recently, several FSS structures have been applied to design Fabry-Pérot cavities [6], [7].

Typically, frequency selective surfaces are designed by changing popular designs or classical topologies and usually involve a process of "trial and error" to get the desired results. The most critical step in the design process of the desired FSS is the proper choice of elements for the array. The element type and geometry, substrate parameters, presence or absence of superstrates, and inter-element spacing, in general, determine the overall frequency response of the structure, such as bandwidth (BW), transfer function, and dependence on the incidence angle and polarization [8]. A comprehensive review of FSS designs is provided in [4].

However, to address the real challenges and requirements presented by nowadays wireless systems, there is a need to develop new solutions and strategies for the design of FSS, antennas, and radio frequency (RF) printed circuits. Moreover, one of these challenges is the development of structures capable of changing the behavior of the operation dynamically and efficiently.

One of the most efficient approaches proposed to design new integrated circuit structures systematically is the integration of electromagnetic analysis software, as the High-Frequency Structure Simulator (HFSS) commercial software, with different optimization techniques [9].

Optimization algorithms as particle swarm optimization (PSO), genetic algorithms (GAs), and artificial neural networks (ANNs), have been widely used for the design and development of microwave passive printed circuits [10], [11].

Brazilian Microwave and Optoelectronics Society-SBMO *received 22 Nov 2018; for review 22 Nov 2018; accepted 25 Feb 2019*
Brazilian Society of Electromagnetism-SBMag *ISSN 2179-1074*

Although the integration between the optimization and electromagnetic analysis algorithms provides a wide design possibility, the computational cost becomes high due to the need for a large number of simulations. Therefore, a new concept is presented within the HPSO implementation that aims to enhance the accuracy of the algorithm, thus reducing the number of iterations needed to achieve convergence, resulting in the development of the HPSO-NZ algorithm which is used to synthesize new active reconfigurable FSSs.

The proposed optimization technique is used to design active reconfigurable FSSs with limited size patch elements printed on single dielectric layers, for operation in the S and C bands, of easy manufacture and integration to other microwave circuits. This technique can be used to synthesize other planar circuits, including antennas, filters, directional couplers and matching circuits.

Section II describes the implementation of the algorithm and the use of classic functional testbeds to verify the algorithm performance. To illustrate the application of the HPSO-NZ algorithm, two RFSSs are designed, fabricated, and measured, as presented in Section III. Conclusions are summarized in Section IV.

II. HPSO AND HPSO-NZ ALGORITHMS: IMPLEMENTATION AND VALIDATION

The PSO algorithm is a global optimizer developed with the main objective of simulating the behavior of a flock of birds in search of food in an open field [9]. The birds (particles) would have a personal and social awareness of the best points visited in that field. These birds (particles) would remember the best-seen position from their personal history, and they would know the best-seen position of the entire flock. With this memory, each bird (particle) is driven toward its best-seen position (pbest) and the flock's global best-seen position (gbest) [9].

Using PSO for hybrid optimization problems with both real and binary parameters is suitable and interesting because the operations related to each problem dimension do not depend on information about other dimensions. This independence allows for different dimensions of the same problem to be represented by real or binary values and subjected to the same PSO update scheme.

A. HPSO Implementation

The PSO shares many similarities with evolutionary techniques such as genetic algorithms (GAs). The system is initialized with a population of random solutions and searches for the optimal solution by successive update iterations. However, unlike GA, PSO has no evolutionary operators such as crossover and mutation.

Brazilian Microwave and Optoelectronics Society-SBMO received 22 Nov 2018; for review 22 Nov 2018; accepted 25 Feb 2019
Brazilian Society of Electromagnetism-SBMag *ISSN 2179-1074*

The PSO is based on the principle that each solution can be represented as a particle within a swarm. Each particle has a vector position and velocity, and each coordinate represents a value of a parameter to be optimized. Then for an N-dimensional optimization, each particle will have a position in an N-dimensional space that represents a possible solution to the problem. The underlying implementation of the PSO algorithm is described in a reduced form in Table I since the flowchart of classical PSO can be found in [10]-[12]. The emphasis here is on the several critical steps that requires special attention when dealing with real and binary parts in different manners.

TABLE I. ALGORITHM IMPLEMENTATION OF HPSO-NZ

	REAL PART	**BINARY PART**
$\bar{x} = [\,\bar{r}\,\bar{b}]$	$\bar{r} = \{\boldsymbol{R}_1, \boldsymbol{R}_2\}$	$\bar{b} = \{\boldsymbol{B}_1, \boldsymbol{B}_2, \ldots \boldsymbol{B}_N\}$
p_{best}, g_{best}	Both parts share the same p_{best} and the same g_{best}	
v-update	$\boldsymbol{V}_t = w\boldsymbol{V}_{t-1} + c_1\eta_1(\boldsymbol{P}_{t-1} - \boldsymbol{X}_{t-1}) + c_2\eta_2(\boldsymbol{G}_{t-1} - \boldsymbol{X}_{t-1})$	
Inertia weight	time varying, 0.9-0.4	constant 1.0
V_{max}	$0.1 \times (R_{max} - R_{min})$	6.0
x-update	$\bar{r} = \bar{r}_{t-1} + \bar{v}_{r,t}$	$S(v_{mn,t}) = \frac{1}{1+e^{-v_{mn,t}}}$ $x_{mn,t} = \begin{cases} 1, r_{mn,t} < S(v_{mn,t}) \\ 0, r_{mn,t} \geq S(v_{mn,t}) \end{cases}$
Boundary	Yes	No
NZ - Radius	$0.05 \times (Boundary_{max} - Boundary_{min})$	

Assume each particle in a swarm is represented by an (M + N)-dimensional vector

$$\overline{x} = \{R_1, R_2, \cdots, R_{M,} B_1, B_2, \cdots, B_N\} \tag{1}$$

by cascading M real variables $\{R_M\}$ $(m = 1,2,\cdots,M)$ and N binary variables $\{B_N\}(n = 1,2,\cdots,N)$.

At each iteration, the real part and binary part share the same personal best, the global best and the velocity updating (v-update) equation. The uniqueness of HPSO lies in the position updating (x-update) [13], [14]. In particular, the position of the real part is updated by the vector summation formulated in Table I, and the binary part needs to be updated via the sigmoid transformation $S(v_{mn,t})$ as applied in

Brazilian Microwave and Optoelectronics Society-SBMO received 22 Nov 2018; for review 22 Nov 2018; accepted 25 Feb 2019
Brazilian Society of Electromagnetism-SBMag *ISSN 2179-1074*

regular binary particle swarm optimization (BPSO) [13]. Other suggested optimization such as the inertia weight w and the maximum velocity V_{max} are also provided by Table I. It is worthwhile mentioning that the boundary condition is only applied to the real part, since the x-update in HPSO intrinsically defines no out-of-boundary solutions in a binary space [14].

B. HPSO with Negative Zones

As defined in the updating basic equations of PSO, the information used to update the speed and position of each particle refer to the position of the best particle of the swarm (gbest) and the best position previously obtained by the particle (pbest). Despite creating a strong tendency toward the best search space positions, there is no mechanism to prevent the particles from going through paths that have already been traced by other particles causing computational resource waste. To avoid such behavior, in this work, the concept of negative zones is proposed.

Negative zones (NZ) are regions within the search space where the swarm of particles should not travel. Negative zones, in the context of the search space, would act as the inverse of the global best, but with the significant difference that while the gbest can change at each iteration, the negative zones are saved in a list that increases with each iteration. As the negative zones increase, the swarm's search space becomes increasingly smaller, allowing particles to travel only in the most promising directions. The algorithm determines a new negative zone from the particle with the worst ranking at each iteration. The negative zone radius is calculated using the boundaries of the search space.

If any particle falls into any of these areas their speed and position are recalculated as follows:

$$\mathrm{V_t} = (-1 + \eta_3)\mathrm{V_t} \tag{2}$$

$$\mathrm{X_t} = \mathrm{X_t} + \mathrm{V_t} \tag{3}$$

Where η_3 is a random value between 0 and 1.

In this way, the particle is repelled by the negative zone and gains speed in a new direction proportional to its previous speed. Figure 1 illustrates the effect of negative zones in the way that each particle travels in search of the desired solution.

Brazilian Microwave and Optoelectronics Society-SBMO *received 22 Nov 2018; for review 22 Nov 2018; accepted 25 Feb 2019*
Brazilian Society of Electromagnetism-SBMag *ISSN 2179-1074*

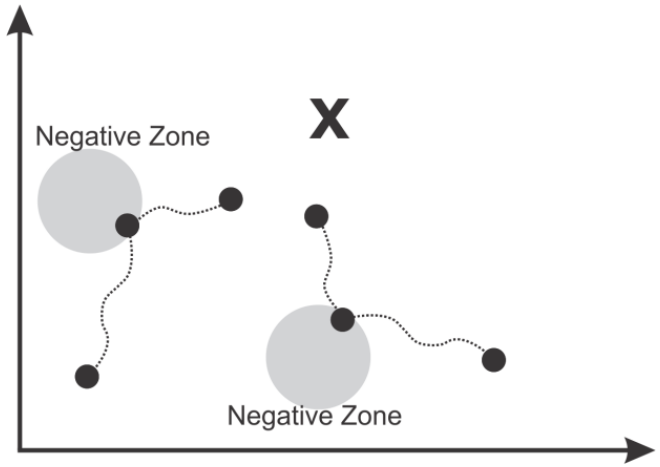

Fig. 1. Description of a swarm that is searching through a 2-D field. Gray circles represent the negative zones and X the optimization objective.

The HPSO-NZ algorithm can be validated by optimizing the Rastrigin function as proposed in [13]. The Rastrigin function is a non-convex function used as a performance test problem for optimization algorithms. It is a typical example of a non-linear multimodal function. Finding the minimum of this function is a somewhat difficult problem due to its large search space and its large number of local minima [14]. The Rastrigin function is defined by [13]:

$$f = \sum_{i=1}^{N} [a_i^2 - 10\cos(2\pi a_i) + 10] \tag{4}$$

In Fig. 2, it is shown an example of Rastrigin function with N = 2, and their overall minimum located at $a_1 = a_2 = 0$.

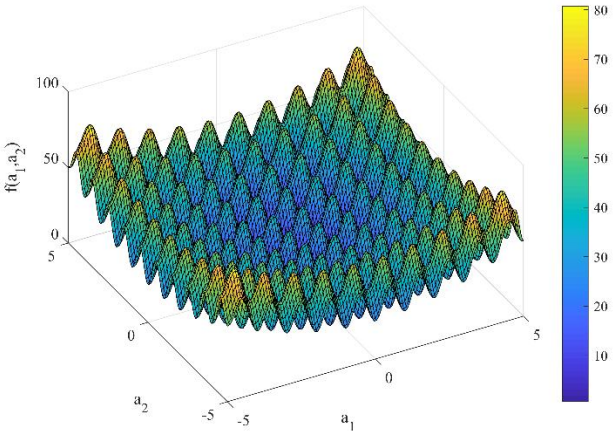

Fig. 2. Topology of the 2-D multimodal Rastrigin function.

  ISSN 2179-1074

In [14] tests were performed with the Rastrigin function using N = 3 to enable a more complex optimization test. The optimizer is a minimizer by default, and the optimization is performed in a search space of 18 dimensions consisting of two real variables $R_1, R_2 \in [-5,5]$ and sixteen binary bits, and according to (4) with $a_1 = R_1$, $a_2 = R_2$, and a_3 is related to the binary part via the mapping:

$$a_3 = \frac{10}{2^{16}-1}\sum_{N=1}^{16} 2^{N-1} \times B_N - 5 \tag{5}$$

where B_N are the binary variables.

Table I shows information on the parameters used in the optimization algorithms.

A swarm of 10 individuals is used on the function optimization for 200 iterations. Due to the stochastic nature of the algorithms, the same test is repeated for 200 independent trials.

The standard HPSO algorithm was used to solve the same problem to compare to previous results. According to [14] a final value lower than 0.5 is considered as an optimal result for the optimization process.

The histogram of Fig. 3 shows the results of 200 independent optimizations performed on the Rastrigin function. Using HPSO-NZ in 169 tests optimum results, less than 0.5, are obtained, while using HPSO only 136 tests returned an optimum value, indicating a difference of approximately 20% between the two algorithms. It is noteworthy that in the 200 HPSO-NZ tests the mean of the results was 0.26 with the standard deviation of 0.38, whereas with the HPSO the mean and standard deviation were 0.56 and 0.50, respectively.

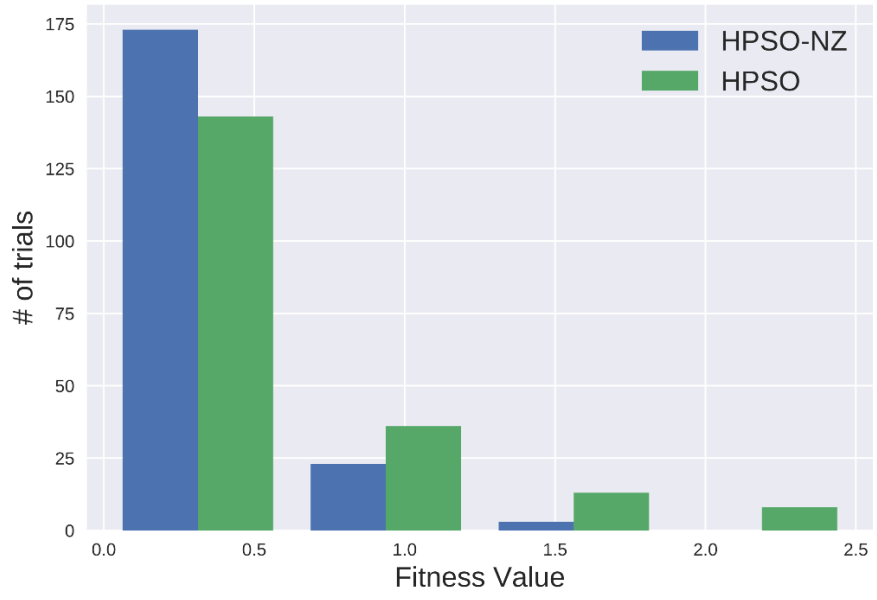

Fig. 3. Histogram of the best fitness values approached in 200 independent trials by HPSO-NZ and standard HPSO.

ISSN 2179-1074

Table II shows a comparison of the HPSO-NZ algorithm with four different algorithms implemented in [14] to solve the same problem.

For a more in-depth validation of our proposal, the HPSO algorithm presented in [14] was also implemented, and it is possible through Table II to verify the reproducibility of the results presented by the authors.

These numerical results indicate that the HPSO-NZ algorithm is more efficient in solving hybrid optimization problems (real/binary) by offering a higher chance of convergence with a smaller number of iterations and particles.

TABLE II. COMPARISON OF 6 COUNTERPART ALGORITHMS (10 PARTICLES, 200 ITERATIONS, 200 TRIALS)

Algorithm	$g_{best} < 0.5$
HPSO-NZ (this work)	**169**
HPSO (this work)	**136**
HPSO [14]	**137**
Binary PSO [14]	**80**
Binary GA [14]	**12**
Round-Off Real PSO [14]	**6**

Furthermore, other aspects of the proposed HPSO-NZ algorithm can pass through other validation processes [15] in order to test other search spaces and to better understand the influence of the hyperparameters on the convergence of the algorithm.

III. RECONFIGURABLE FSS PERIODIC STRUCTURES

A reconfigurable FSS is a structure that can allow or block wave propagation simply by activating or deactivating primary switchers such as diodes.

The basic unit cell of an active FSS structure used in this work is shown in Fig. 4. The diodes are inserted between the parallel discontinuous strips. This unit cell is reproduced in the x-y plane. An electromagnetic wave illuminates the unit cells with an electric field polarized parallel to the strips. It is well-known that an array of parallel continuous wires will act as a high-pass filter which is mainly due to the inductive behavior of the wires [1]. On the other hand, a similar passive array of discontinuous wires shows band rejection filter behavior due to the capacitive effect between the discontinuous elements conjugated in series to the previously considered inductive effect [1], [2].

Figure 4 shows simulated results for a RFSS structure with active elements (PIN diodes). The unit cell is 20 mm x 20 mm, the strip width (W) is 1 mm, and the gap discontinuity dimension (g) is 1 mm. The

Brazilian Microwave and Optoelectronics Society-SBMO *received 22 Nov 2018; for review 22 Nov 2018; accepted 25 Feb 2019*
Brazilian Society of Electromagnetism-SBMag *ISSN 2179-1074*

RFSS transmission coefficient frequency response is depicted assuming that all PIN diodes are forward biased (ON state) or unbiased (OFF state), corresponding to unit cells with continuous or discontinuous conducting strips, respectively. In the HFSS analysis, the OFF state is simulated by replacing each PIN diode by a capacitor of 0.17 pF. In the ON state, each diode is replaced by a 2.1 Ω resistor.

In order to achieve different frequency responses, it is necessary to change the cell unit shown in Fig. 4. In the optimization process, the active FSS analysis and synthesis is performed without using (at the beginning) any basic patch element geometry.

The hybrid optimization approach was chosen because it allows the cell dimensions (W_x and W_y) to be encoded as integer values and the patch geometry as a binary string. Without the constraint of specific geometry, the algorithm can obtain an entirely new patch configuration for the problem.

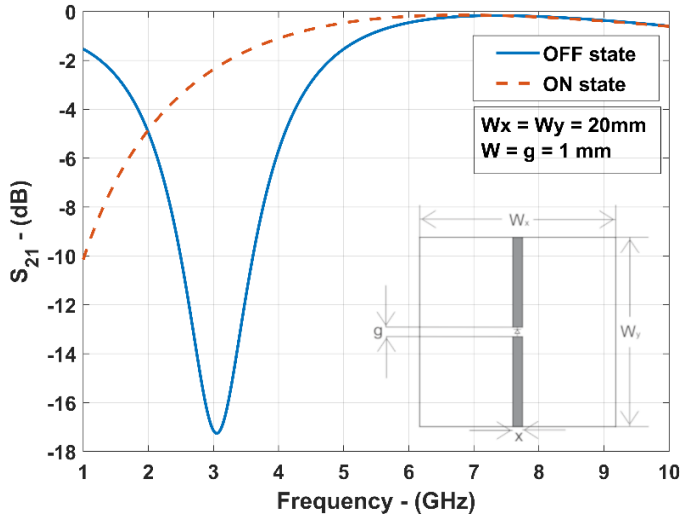

Fig. 4. Simulation results for the transmission coefficient frequency response of the RFSS with PIN diodes and the illustrated unit cell. All PIN diodes are biased (ON state), for continuous strips, or unbiased (OFF state), for discontinuous strips.

Figure 5 illustrates the concept of a primary FSS structure divided into small patches that can be optimized to create the necessary configuration for the desired FSS frequency response.

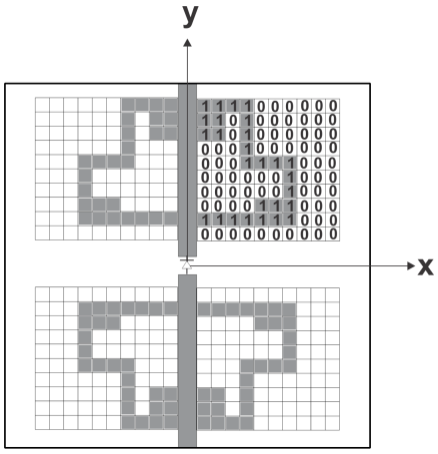

ISSN 2179-1074

Fig. 5. Concept of a binary FSS structure with patch elements.

A. Optimized Reconfigurable Frequency Selective Surfaces

Using the HPSO-NZ algorithm with the constraints summarized in Table III, the algorithm started with the goal of creating a new geometric configuration to operate as a band-pass filter at the 7 GHz band, when all the PIN diodes are on the OFF state, and to behave as a stopband filter at this frequency band, when all diodes are on the ON state. The algorithm converged after 600 iterations. Figure 6 shows an illustration of the internal patches' configuration ("pixels") of the synthesized RFSS with 20 mm x 20 mm unit cells.

TABLE III. OPTIMIZED RFSS DESIGN GOALS AND STRUCTURAL PARAMETERS

OPTIMIZED FSS PARAMETERS	**VALUES**
MAXIMUM RECTANGULAR CELL WIDTH (mm), W_X	100
MAXIMUM RECTANGULAR CELL LENGTH (mm), W_Y	100
MINIMUM RECTANGULAR CELL WIDTH (mm), W_X	10
MINIMUM RECTANGULAR CELL LENGTH (mm), W_Y	10
FREQUENCY DESIGN GOAL (GHz), F	7.0
SUBSTRATE LAYER RELATIVE PERMITTIVITY (FR4), ε_r	4.4
SUBSTRATE LAYER LOSS TANGENT, $tan\delta$	0.02
SUBSTRATE LAYER HEIGHT (mm), h_1	1.57
NUMBER OF INTERNAL PATCHES ("PIXELS")	400
NUMBER OF PATCHES USED IN HPSO-NZ	100
DIMENSIONAL PROBLEM SPACE	2100
SWARM SIZE	20
MAXIMUM ITERATION NUMBER	600

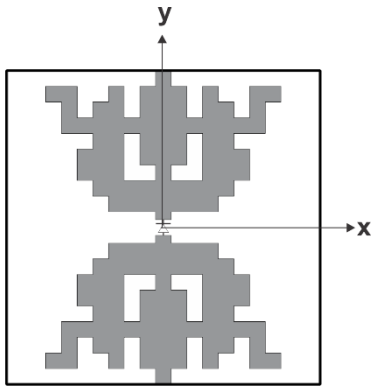

Fig. 6. Illustration of the RFSS patch element with a central air gap (1 mm x 1 mm) to integrate a PIN diode.

The HPSO-NZ algorithm optimized configuration was used to fabricate a RFSS prototype with Infineon BAR64-03W PIN diodes, 20 cm x 20 cm overall size, and 100 cells. Figure 7 shows photographs

  ISSN 2179-1074

of the fabricated prototype. Conducting strips are used to ensure that all the RFSS PIN diodes would be connected to the feed line on the ON state, as shown in Fig. 7(b).

Furthermore, the proposed HPSO-NZ algorithm synthesized a RFSS with 20 mm x 20 mm unit cells and the configuration of internal patches ("pixels") shown in Fig. 7(a).

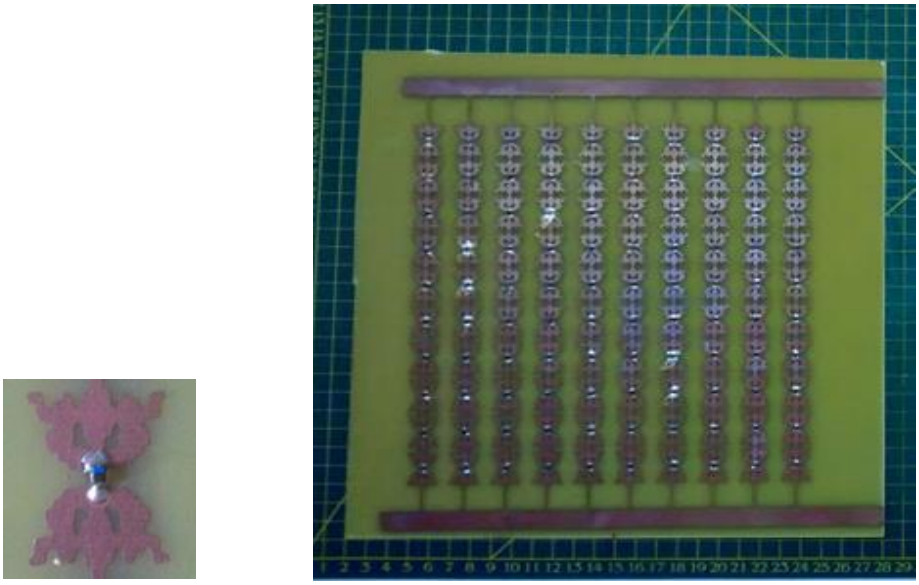

(a) (b)

Fig. 7. Photographs of the RFSS prototype. (a) Unit cell and (b) array.

Simulation and measurement results for the frequency response of the RFSS transmission coefficient are presented in Fig. 8, for both ON-state and OFF-state, for comparison purpose. Infineon BAR64-03W PIN diodes [16], [17], are used to enable the FSS reconfigurability.

As shown in Fig. 8, the optimized RFSS, with all diodes on the OFF state, presents a stopband performance with simulated and measured bandwidth results of about 1.5 GHz and 1.9 GHz, respectively, for a -10 dB reference level. Similarly, the optimized RFSS, with all diodes on the ON state, presents a bandpass performance with simulated and measured bandwidth results of about 3.8 GHz and 1 GHz, respectively, for a -3 dB reference level. In addition, the difference between the FSS transmission coefficients at the center frequency, in both cases (ON and OFF states), is greater than 15 dB.

Brazilian Microwave and Optoelectronics Society-SBMO *received 22 Nov 2018; for review 22 Nov 2018; accepted 25 Feb 2019*
Brazilian Society of Electromagnetism-SBMag *ISSN 2179-1074*

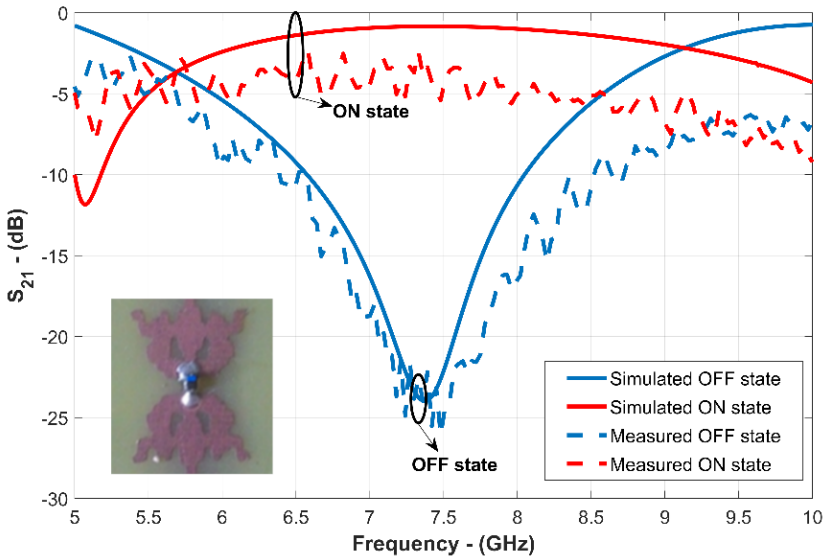

Fig. 8. Simulation and measurement results for the transmission coefficient versus frequency of the optimized FSS.

To further test the proposed optimization algorithm for different conditions, another optimization problem is carried out with new constraints and objectives. The optimized RFSS should operate as a stopband filter at the 3 GHz band, when all the PIN diodes are on the OFF state and present two rejection bands at 2 GHz and 4 GHz, but not at 3 GHz, when all the PIN diodes are on the ON state.

To reduce the FSS fabrication complexity observed in the fabrication of the first RFSS prototype, shown in Fig. 7, the number of internal pixels was reduced to 100 "pixels". Once again, Infineon BAR64-03W PIN diodes [16], [17], are used to enable the FSS reconfigurability. After using the same algorithm constraints summarized in Table I, the algorithm has been started and converged after 600 iterations with a 60 mm x 60 mm unit cell. Figure 9 shows an illustration of the internal patches' configuration ("pixels") of the synthesized RFSS.

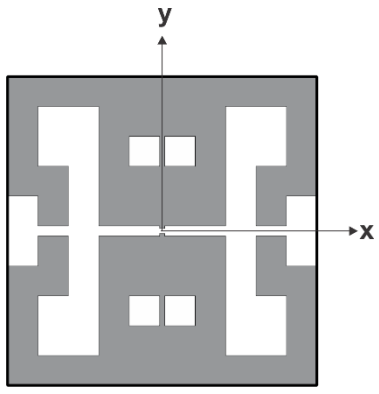

Fig. 9. Illustration of the RFSS unit cell and patch element with central air gap to integrate a PIN diode.

Brazilian Microwave and Optoelectronics Society-SBMO *received 22 Nov 2018; for review 22 Nov 2018; accepted 25 Feb 2019*
Brazilian Society of Electromagnetism-SBMag *ISSN 2179-1074*

The HPSO-NZ algorithm optimized configuration was used to fabricate a RFSS prototype with Infineon BAR64-03W PIN diodes, 20 cm x 20 cm overall size, and 16 cells. Again, the algorithm was able to propose a patch geometry that exhibits the desired behavior. Figure 10 shows photographs of the fabricated prototype.

The experimental results were measured at the GTEMA/IFPB Microwaves Laboratory, using an Agilent two ports network analyzer, N5230A, and two 20 dB standard horn antennas. The PIN diodes are activated using a controlled power supply to avoid any risk of damage to the circuits. Two feeding lines have been added to the structure to allow the diodes biasing as shown in Fig. 10(b).

Furthermore, the proposed HPSO-NZ algorithm synthesized a RFSS with 20 mm x 20 mm unit cells and the configuration of internal patches ("pixels") shown in Fig. 10(a).

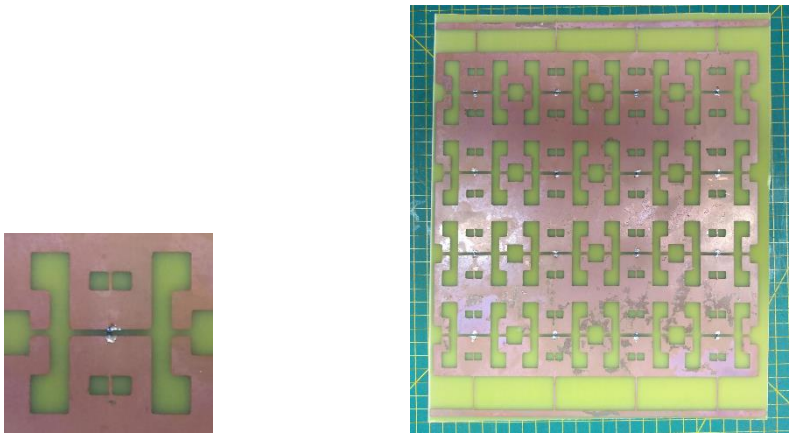

(a) (b)

Fig. 10. Photographs of the RFSS prototype. (a) Unit cell and (b) array.

Simulation and measurement results for the frequency response of the RFSS transmission coefficient are presented in Fig. 11, for both ON-state and OFF-state, for comparison purpose. Infineon BAR64-03W PIN diodes [16], [17], are used to enable the FSS reconfigurability.

As shown in Fig. 11, the optimized RFSS, with all diodes on the OFF state, presents a stopband performance with simulated and measured resonant frequency (and bandwidth) results of about 3.2 GHz (BW = 3.3 GHz) and 3.05 GHz (BW = 3 GHz), respectively. Similarly, the optimized RFSS, with all diodes on the ON state, presents an stopband performance with two resonance bands with simulated and measured resonant frequency results of about 1.9 GHz and 2 GHz, for the first resonance, and of about 4.2 GHz and 4.3 GHz, respectively.

Brazilian Microwave and Optoelectronics Society-SBMO *received 22 Nov 2018; for review 22 Nov 2018; accepted 25 Feb 2019*
Brazilian Society of Electromagnetism-SBMag *ISSN 2179-1074*

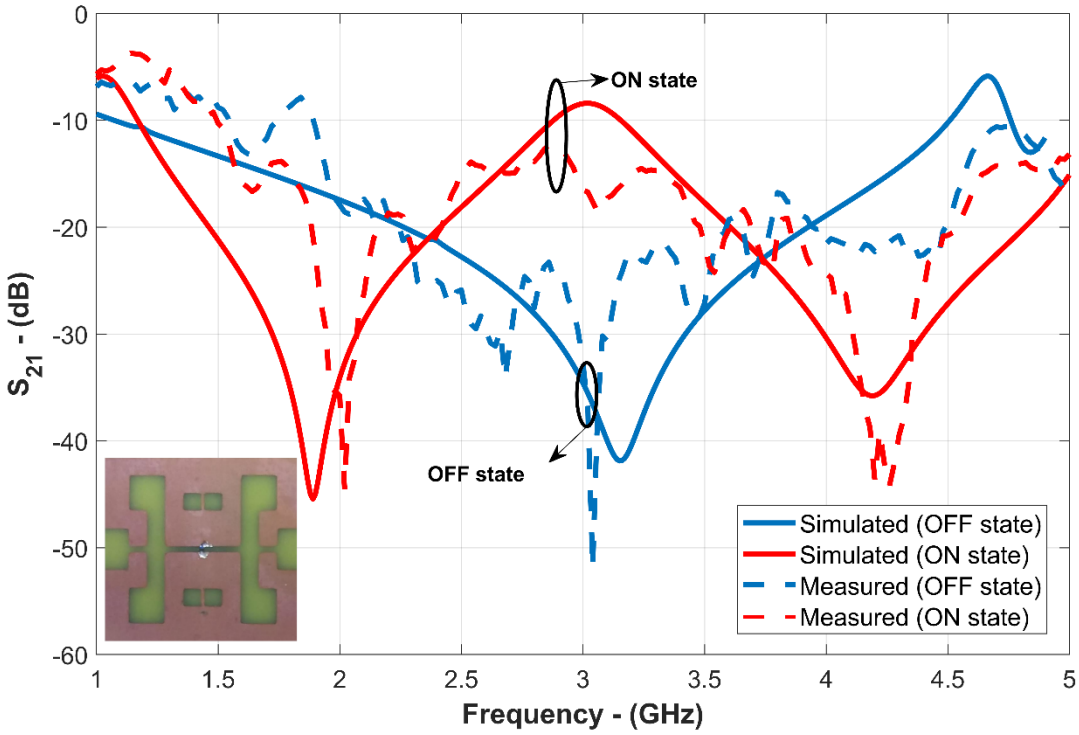

Fig. 11. Simulation and measurement results for the transmission coefficient versus frequency of the optimized FSS.

As shown in Fig. 11, the RFSS bandwidth results at the two measured resonance bands (2 GHz and 4.3 GHz) are greater than 1.5 GHz in both cases, with all diodes on the ON or OFF states. In addition, at 3 GHz and (with all diodes on the ON or OFF states) the RFSS transmission coefficient result has increased in about 32 dB in both cases, confirming that the optimized RFSS structure has accomplished the main goals in changing its frequency behavior.

IV. CONCLUSION

This paper presented a new variation of the PSO algorithm that is even more robust and able to achieve optimal results using a smaller set of particles than classical (HPSO, Binary PSO, Binary GA, and Round-Off Real PSO) algorithms.

The developed HPSO-NZ algorithm was used in the synthesis of two RFSS structures with limited size patch elements and PIN diodes to achieve frequency reconfigurability for applications in S- and C-microwave bands. In one case, the FSS performance was electronically changed from stopband to

received 22 Nov 2018; for review 22 Nov 2018; accepted 25 Feb 2019

ISSN 2179-1074

bandpass (at the same resonant frequency) and, in the other case, the RFSS performance was changed from single-band to dual-band.

Two RFSS prototypes are fabricated and measured. The RFSS transmission coefficient simulation and measurement results, for both forward (ON state) and reverse (OFF state) bias, are compared showing a good agreement. It is observed that the proposed RFSS optimization model is innovative and can be used in the development of other planar microwave circuits, such as antennas, filters, power dividers, and couplers for embedded and limited size circuit applications.

The use of the HPSO-NZ algorithm provided unique conducting patch configurations for the RFSS patch elements, which are different from the usual Euclidean and fractal geometries, with the possibility of defining structural symmetries and asymmetries.

However, it is important to point out that there is a greater complexity of implementation that must be observed with attention since small changes can influence the convergence of the optimization process. Another drawback of the algorithm is the inclusion of a new hyperparameter to be adjusted. In addition, comparisons of optimization results of a classical problem were presented to validate the proposed changes and highlight the benefits of the new algorithm.

ACKNOWLEDGMENTS

This work was supported by CNPq under covenant 573939/2008-0 (INCT-CSF), Federal Institute of Paraíba (IFPB), and Federal University of Rio Grande do Norte (UFRN).

REFERENCES

[1] M. A. Habib, M. N. Jazi, A. Djaiz, M. Nedil, and T. A. Denidni, "Switched-beam antenna based on EBG periodic structures," IEEE MTT-S Int. Microw. Symp. Dig., Boston, MA, 2009, pp. 813-816.

[2] C. G. Christodoulou, Y. Tawk, S. A. Lane, and S. R. Erwin, "Reconfigurable antennas for wireless and space applications," *Proc. IEEE*, vol. 100, no. 7, pp. 2250-2261, 2012.

[3] Y. Tawk, J. Constantine, and C. Christodoulou, "Reconfigurable Filtennas and MIMO in Cognitive Radio Applications," *IEEE Trans. Antennas Propag.*, vol. 62, no. 3, pp. 1074-1083, 2014.

[4] B. A. Munk, Frequency Selective Surfaces, John Wiley & Sons, NY, 2000.

[5] M. A. Habib, M. N. Jazi, A. Djaiz, M. Nedil, and T. A. Denidni, "Switched-beam antenna based on EBG periodic structures," IEEE MTT-S Int. Microw. Symp. Dig., Boston, MA, 2009, pp. 813-816.

  ISSN 2179-1074

[6] D. B. Brito, A. G. D'Assunção, R. H. C. Maniçoba, and X. Begaud, "Metamaterial-inspired Fabry–Pérot antenna with cascaded frequency selective surfaces", *Microw. Opt. Technol. Lett.*, vol. 55, pp. 981–985, 2013.

[7] M. Abdelghani, H. Attia, and T. A. Denidni, "Dual- and wide-band Fabry-Pérot resonator antenna for WLAN applications," *IEEE Antennas Wireless Propag. Lett.*, 2016.

[8] K. Sarabandi and N. Behdad, "A frequency selective surface with miniaturized elements," *IEEE Trans. Antennas Propag.*, vol. 55, no. 5, pp. 1239-1245, 2007.

[9] Y. Rahmat-Samii, J. M. Kovitz, and H. Rajagopalan, "Nature-inspired optimization techniques in communication antenna designs," *Proc. IEEE*, vol. 100, no. 7, 2012.

[10] N. Jin and Y. Rahmat-Samii, "Advances in particle swarm optimization for antenna designs: Real-number, binary, single-objective and multiobjective implementations," *IEEE Trans. Antennas Propag.*, 2007.

[11] P. H. F. Silva, P. Lacouth, G. Fontgalland, A. L. P. Campos, and A. G. D'Assunção, "Design of frequency selective surfaces using a novel MoM-ANN-GA technique," Proc. SBMO/IEEE MTT-S Int. Microwave Optoelectronics Conf., Salvador, Brazil, 2007, pp. 275-279.

[12] J. Kennedy and R. Eberhart, Swarm Intelligence, New York: Morgan Kaufmann, 2001.

[13] J. Kennedy and R. Eberhart, "Particle swarm optimization," Proc. IEEE Int. Conf. Neural Networks, Perth, Australia, 1995, pp. 1942-1948.

[14] N. Jin and Y. Rahmat-Samii, "Hybrid Real-Binary Particle Swarm Optimization (HPSO) in Engineering Electromagnetics," IEEE Transactions on Antennas and Propagation, vol. 58, no. 12, pp. 3786-3794, December 2010.

[15] K. A. De Jong, "An analysis of the behavior of a class of genetic adaptive systems", Ph.D. thesis, University of Michigan, 1975.

[16] Infineon Technologies. (2015, Mars) Infineon. [Online]. http://www.infineon.com/dgdl/Infineon-BAR64SERIES-DS-v01_01-en.pdf?fileId=db3a304314dca3890114fef8f4ca0aca

[17] Skyworks. (2016, September) [Online]. http://www.skyworksinc.com/uploads/documents/200051J.pdf

received 22 Nov 2018; for review 22 Nov 2018; accepted 25 Feb 2019

ISSN 2179-1074